ELSEVIER

Thermochimica Acta 359 (2000) 143–159

thermochimica acta

www.elsevier.com/locate/tca

Experimental study of multiple glass transitions within a material

S.S.N. Murthy*

School of Physical Sciences, Jawaharlal Nehru University, New Delhi 110067, India

Received 20 January 2000; accepted 16 April 2000

Abstract

A detailed study of the relaxation in the supercooled plastic crystalline phase has been carried out using dielectric spectroscopy and differential scanning calorimetry in *cis*-1,2 dimethylcyclohexane, neopentanol, cyclopentanol and a number of cyclohexyl derivatives to resolve the ambiguity regarding the glass transition temperatures, and the spectral shape. The various transitions (and the associated enthalpies) along with the glass transition temperature corresponding to the supercooled plastic phase are determined. The shape of the relaxation spectra and the temperature dependence of the relaxation rate are found to follow the strong and fragile pattern of Angell. Because of the difficulty in supercooling the liquid phase, the liquid–glass transition temperatures are determined in an indirect way using binary solution method. These transition temperatures are found to be about 6–9° above that of the plastic crystal to 'glass' transition temperatures.

Keywords: Multiple glass transitions; Differential scanning calorimetry; Dielectric spectroscopy; Plastic crystals

1. Introduction

The glassy state [1,2] that is obtained by supercooling a melt below its freezing temperature (T_m) is a result of the freezing of certain degrees of freedom rather sharply at the glass transition temperature T_g. These degrees of freedom, depending on the molecular structure, are a complicated combination of positional, rotational and internal degrees of freedom. In this context quite often, interesting examples are provided by frozen states of various intermediate phases such as plastic [3–5] and liquid [6,7] crystals. The former can be recognized as positionally ordered in the three-dimensional lattice, but orientationally disordered. The disorder can be brought into a frozen state if the crystal is cooled rapidly enough to prevent transformation into the low temperature ordered phase. This new kind of vitreous state exhibits characteristic features of glassiness related to orientational degrees of freedom. The term ''glassy crystal'' is suggested [8] for this category of state of aggregation and ''glassy liquid'' for the frozen state of the supercooled isotropic liquid. To avoid possible confusion, we use the notation $T_g(pc)$ (T_g of the plastic crystalline phase) for the former and $T_g(l)$ for the latter throughout this article.

Since only the orientational degrees of freedom are involved, the study of the relaxation of the supercooled plastic phase is expected to give some important clues to the understanding of the glass transition phenomena. With this in mind, dielectric study has been performed in ethanol [9,10], cyclooctanol [11,12], 1-cyanoadamantane [13–15] and cyclohexanol [4,16]. The relaxation spectra corresponding to the supercooled plastic phase has been found to be

* Tel.: +91-11-6189701; fax: +91-11-6194137.
E-mail address: ssnm@jnuniv.ernet.in (S.S.N. Murthy)

0040-6031/00/$ – see front matter
PII: S0040-6031(00)00522-0

non-Debye and the temperature dependence of the corresponding relaxation rate is non-Arrhenius, as in supercooled liquids [18]. In contrast to this general behaviour the relaxation in the plastic phases of neohexanol [19], neopentanol [19] and cyclopentanol [20] appears to be Arrhenius and the corresponding spectral behaviour to be Debye; which is not generally found in condensed systems with the exception [18] of simple alcohols. Apart from this, conflicting $T_g(\mathrm{pc})$ values are reported by various researchers [19,21,22] for these systems. In this context, in the light of the results on ethanol [23] and cyclohexene [8] where the $T_g(\mathrm{l})$ and $T_g(\mathrm{pc})$ values are reported to be the same, it is not clear whether this is the case with the other materials as well. However, because of the requirement of very high cooling rates, the liquid–glass formation in the materials which show plastic crystalline phase is often not easy. Angell et al. [24] used binary solution data to find $T_g(\mathrm{l})$ by extrapolation and in the case of cyclohexanol the $T_g(\mathrm{l})$ is found to be about 10° above $T_g(\mathrm{pc})$. Hence, this communication is aimed at resolving the above ambiguities regarding the T_g's by critically examining the above systems along with some of the cyclohexane derivatives (which impart a variety of shapes to the molecule) with the help of differential scanning calorimetry (DSC) and dielectric spectroscopy.

2. Experimental

The samples investigated are given below along with the code used for further discussion in the paper. The samples are cyclopentanol or CP.OH (99% purity); 2,2 dimethylpropanol or neopentanol or NP.OH (99%); *cis*-1,2 dimethylcyclohexane or DMCH (99%); cyclohexylchloride or CH.Cl (99%); cyclohexylbromide or CH.Br (98%); cychohexyliodide or CH.I (98%), all obtained from Aldrich, USA; cyclohexanone or CH.O (synthesis grade) from E. Merek, India; cyclohexanol or CH.OH (AR), s.d. fine, India. The solvents used for binary solution data are propyleneglycol or PG (LR, s.d. fine, India), isopropylbenzene or IPB (99%, Aldrich), ethanol or EOH (GR, E. Merck, Germany) and dioctylphthallate or DOP (LR, Ranbaxy, India). All these chemicals are used as received.

The DSC measurements are made using a Du Pont TA 2000 thermal analyzer using the quench cooling accessory. For the dielectric measurements, a HP 4284A Precision LCR meter in the frequency range 20 Hz–1 MHz is used. The DC step-response technique is used for the measurements of dielectric loss at ultralow frequencies. For the other details of the experimental set-up and for the accuracy in the measurements the reader may consult the earlier articles [7,18,25] from this laboratory.

3. Results

For the sake of clarity the results are briefly summarized below and the sample-wise details are given later.

3.1. Transition temperatures

The stable transition temperatures are measured using DSC technique for a heating rate of 2 K/min after annealing the samples at the appropriate crystallization zones. The enthalpies associated with the transitions are measured [25] with the help of the DSC analysis software. These are listed in Table 1 along with the literature values (determined for some of the samples) to give the reader some confidence in the present work. The nature of the transitions based on the DSC and dielectric studies is also listed. The results given in Table 1 are an average of atleast five runs.

3.2. Measurement of $T_g(\mathrm{pc})$

The glass transition in the plastic phase event is not seen in the DSC curves in all the samples cooled at a rate of 10 K/min except for DMCH and CH.OH. Therefore, very high cooling rates of the order 200–800 K/min are used by dipping the sample pans directly into liquid nitrogen [7]. The sample pans are then introduced into the DSC cell at 100 K and heated at a rate of 10 K/min after equilibration. (For the sake of convenience, this method is referred to as fast quench cooling (FQC). The reader is referred to [7] for further details.) For samples which are not in their plastic phase at room temperature, the above method is executed by taking the sample pans from the DSC cell held isothermally at temperatures corresponding to the plastic phase. Even for these high

Table 1
Details of various transition temperatures

Sample	Nature of transition[a]	Transition temperature (K)			ΔH(kJ/mole)		
		Present work	Literature		Present work	Literature	
				References			References
CP.OH	SI→L	253.3	256.0		1.53	1.54	
	SII→SI	235.2	236.4	[26]	0.09	0.11	[26]
		226.0 (M)	–		–	–	
	SIII→SII	201.8	202.5	–	2.95	3.71	
		200.4			0.77		
	SIV→SIII	199.4 (M)	–	–	–	–	–
	SV→SIV	170 (M)	–	–	–	–	–
	SVI→SV	161.8 (M)	–	–	–	–	–
NP.OH	SI→L	329.3	330.0		5.75	–	
	SII→SI	236.5	229	[29]	4.54	–	
DMCH	SI→L	224.5	223.2		–	1.65	
	SII→SI	–	172.5	[5]	–	8.26	[5]
CH.Cl	SI→L	229.1	229.3	[27,28]	1.78	2.04	[28]
	SII→SI	220.6	220.4		7.93	8.01	[28]
	SIII→SII	–	120.0		–	0.050	[28]
CH.Br	SI→L	217.0	216.7	[29]	10.87	–	–
CH.I	SI→L	229.6	–	–	10.93	–	
CH.O	SI→L	241.5	242.0	[26]	0.87	1.0	
	SII→SI	221.0	224.8		7.85	8.7	[26]

[a]S: crystalline solid, L: liquid, M: Metastable.

cooling rates the glass transition is found to be partial for CP.OH, NP.OH and CH.Cl, as the samples crystallized into some metastable phases. (On using FQC, CH.Br appears to form a metastable plastic phase which is partially supercooled during FQC.) After carefully studying the DSC curves for various cooling and heating rates and also by annealing the samples at appropriate temperatures, the glass transition temperatures and the metastable phases are identified. The results of $T_g(\mathrm{pc})$ are tabulated in Table 2 which are actually an average of atleast five runs. No glass transition event is noted in CH.O.

Table 2
Details of T_g's, T_b/T_m and T_b/T_c[a]

Sample	T_b (from Ref. [29])	T_m	T_c[b]	$T_g(\mathrm{l})$	$T_g(\mathrm{pc})$	$T_m/T_g(\mathrm{l})$	$T_c/T_g(\mathrm{pc})$	T_b/T_m	T_b/T_c
CH.I ($C_6H_{11}I$)	>453.2	229.6	–	140.1	–	1.630	–	>1.97	–
CH.Br ($C_6H_{11}Br$)	439.4	217.0	M[c]	130.5	124.3	1.663	–	2.025	–
CH.Cl ($C_6H_{11}Cl$)	416.2	229.1	220.6	126.0	118.1	1.818	1.868	1.817	1.887
CH.O ($C_6H_{12}O$)	428.0	241.5	221.0	126.0	–	1.917	–	1.772	1.937
CP.OH ($C_5H_{10}O$)	414.0	253.3	201.8	137.7	128.5	1.971	1.570	1.634	2.052
NP.OH ($C_5H_{11}OH$)	386.0	329.3	236.5	145.5	139.3	2.263	1.698	1.172	1.632
CH.OH ($C_6H_{12}O$)	434.2	298.0	245.0	158.6	150.8	1.879	1.625	1.457	1.772
DMCH (C_8H_{16})	397.0	224.5	172.5	–	107.8	–	1.600	1.768	2.301

[a]All temperatures in degrees Kelvin.
[b]T_c is the equilibrium temperature corresponding to the rigid–plastic crystal transition as shown in Fig. 5 which may readily be identified with SII → SI or SIII → SII transition in Table 1.
[c]Metastable.

3.3. Measurement of $T_g(l)$

Of the non-plastic crystalline samples, only CH.I forms liquid–glass easily even for a cooling rate of 10 K/min. The rest of the liquid samples quickly solidify to their plastic phase even on using FQC, though some of the samples show a tendency for partial liquid–glass formation, as a smeared (small) glass like transition (just above $T_g(pc)$) in DSC curves. However, it is very difficult to justify this event as due to the liquid–glass alone as partial glassy crystal formation is also possible. For this reason an indirect method of estimating the $T_g(l)$ by extrapolation of the binary solution data is used. Usually $T_g(l)$ of a binary liquid follows the equation [30,31]:

$$T_g(l)\ \ (\text{mixture}) = T_{g1}(l)(1-x) + T_{g2}(l)x + k'x(1-x) \quad (1)$$

where the T_g's are the liquid–glass transition temperatures of the pure-component liquids, x the weight fraction of the second component and k' is the interaction parameter. Eq. (1) is found [31,32] to be valid for substances that do not form complexes [33,34], and also for many polymer-plasticizer systems [30] and simple binary liquids [31,32]. Taking the second component as the sample whose $T_g(l)$ is required (i.e., $T_{g2}(l) = T_g(l)$), the $T_g(l)$ of the mixture is measured for different values of the weight fraction x of the sample in the binary. After trying a number of liquids the first component liquid is chosen to be atleast two of the liquids, chosen from PG, IPB, EOH and DOP for easy glass formation over a comfortable range of x. And also the first component liquids are chosen in such a way that the $T_{g1}(l)$ is above and below $T_{g2}(l)$ so that one can make extrapolations from both above and below $T_{g2}(l)$ so as to minimize the uncertainty in the extrapolations. The usefulness of Eq. (1) is clearly seen in the case of CH.I (which is a good glass former on its own), where the line given by Eq. (1) smoothly ends at the measured $T_g(l)$ (Fig. 6(c)). The fits to Eq. (1) are given in Fig. 6 and Table 3; and the final results are entered in Table 2. (It must be mentioned in this context that with increase in x especially for $x > 0.5$, FQC method is required for complete glass formation (without any intervention of crystallization)). It is believed that the $T_g(l)$ values thus determined are accurate to ± 0.5 K in most of the cases. Some important results of DSC are given in Figs. 1, 2 and 6–11.

3.4. Dielectric relaxation measurements

The purpose of the dielectric measurements is to see: (i) the spectral shape of relaxation corresponding to the stable plastic phase (and also its supercooled state); (ii) to examine the T-dependence of the relaxation frequency; (iii) to see whether the $T_g(pc)$ measured in the DSC experiment, corresponds to the kinetic freezing of the process. The plastic phases of all the H-bonded systems show a dispersion in the LCR bridge frequency range below 253 K and measurements can be extended into the supercooled plastic phase by a few degrees. With DMCH, the measurements could easily be extended to T_g. However, in the case of other samples, the dielectric dispersion occurs much above the present frequency

Table 3
Details of the fits to Eq. (1)

First component	Second component	T_{g1} (K)	T_{g2} $(= T_g(l))$ (K)	k'
IPB	CH.I	135.4	140.1	−8
IPB	CH.Br	135.4	130.5	10
IPB	CH.Cl	135.4	126.5	+5
DOP	CH.Cl	187.3	126.5	−15
IPB	CH.O	135.4	126.0	20
EOH	CP.OH	98.0	137.0	−4
PG	CP.OH	172.0	138.3	4
IPB	CP.OH	135.5	144.0	−15
EOH	NP.OH	96.0	145.5	−4
PG	NP.OH	171.5	145.5	15
PG	CH.OH	172.9	158.6	0

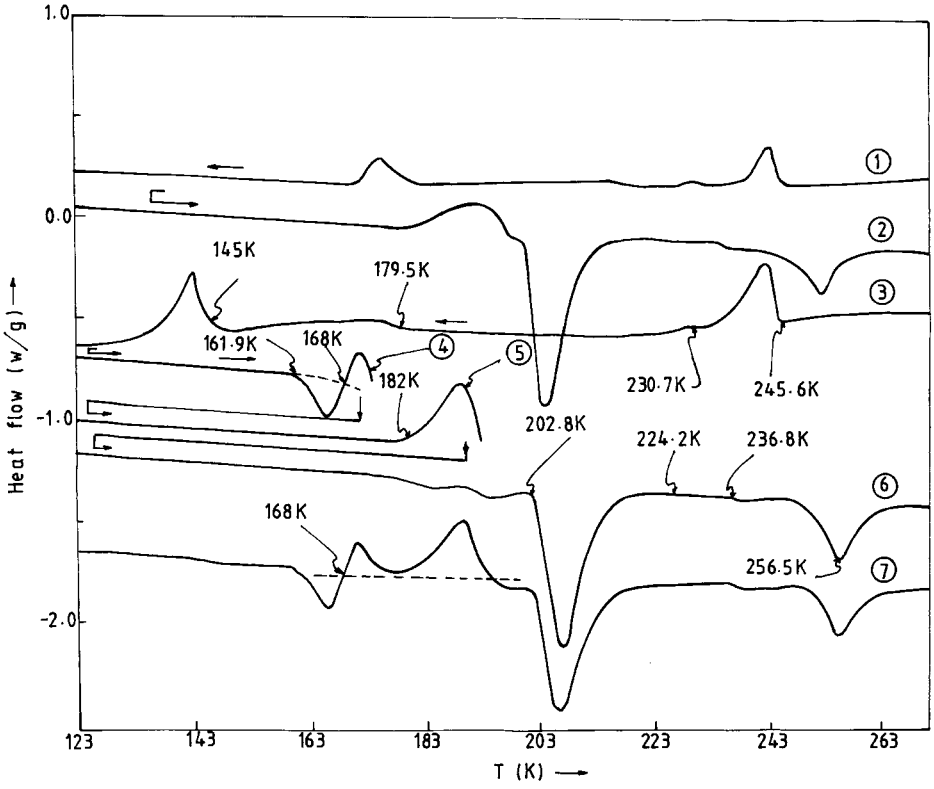

Fig. 1. DSC curves of CP.OH recorded during cooling and heating as indicated by the direction of the arrow. Curve (1) is for sample during cooling at a rate of approximately 5 K/min; (2) is the corresponding heating curve at the same rate; (3) is for sample cooled at a rate of 20 K/min during cooling; (4)–(6) are the heating curves at a rate of 10 K/min for the same sample with different thermal histories as shown by the arrows (sample size=15.8 mg). Curve (7) is recorded during heating of the sample cooled at a rate of 20 K/min.

range and not much could be achieved other than what is already published. The shape of the dielectric spectra for the samples NP.OH, CH.OH and DMCH can well be described by the Hevriliak–Negami (HN) equation [33,35]:

$$\frac{\epsilon^*(f) - \epsilon'_\infty}{\epsilon_0 - \epsilon'_\infty} = \left[1 + \mathrm{i}\left(\frac{f}{f_{\mathrm{HN}}}\right)^{1-\alpha}\right]^{-\beta} \tag{2}$$

where α, β are the geometrical shape parameters, f_{HN} the mean relaxation frequency and ϵ_0, ϵ'_∞ are the static- and the high frequency-limits of the dispersion, respectively. In Eq. (2) ϵ'_∞ is always found to be much above the actual infinite frequency limit ϵ_∞ (equal to $1.05n_{\mathrm{D}}^2$, where n_{D} is the refractive index at the optical frequencies). The dispersion data is summarized in Fig. 3 in the form of normalized Cole–Cole (C–C) diagram; where one can see that Eq. (2) is valid over most part of the C–C diagram, except for the case of CP.OH. The T-dependance of peak loss frequency f_{m} is obtained from f_{HN}, α and β as described in the recent publication [33]. Approximate values of f_{m} deep inside the supercooled region are also obtained by taking measurements very quickly in the partially crystallized sample. In CH.OH, the complete glassy state could be obtained by rapidly cooling the plastic sample by dipping the dielectric cell into liquid nitrogen, and the dielectric data in the ultra low frequency region are then obtained [16] at temperatures near $T_{\mathrm{g}}(\mathrm{cry})$ using DC step-response technique. The temperature variation of the dielectric strength ($\Delta\epsilon = \epsilon_0 - \epsilon_\infty$) for these four samples is shown in Fig. 4. The f_{m} values measured are plotted against $T_{\mathrm{g}}(\mathrm{pc})/T$ in Fig. 5. The f_{m} values obtained for the

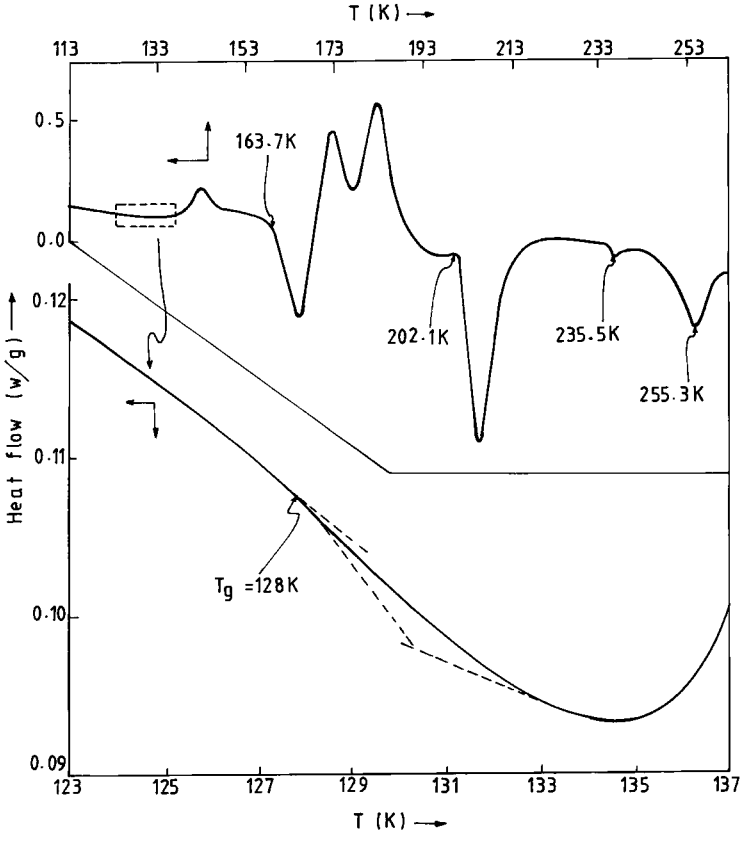

Fig. 2. DSC curve recorded for CP.OH during heating at a rate of 10 K/min for a sample that is fast quench cooled (FQC) from its plastic crystalline phase (sample size=13.5 mg). The inset shows the blown-up portion of the part of DSC curve around T_g(pc). Note that there is a crystallization peak located around 140 K; immediately above the glass transition event at 128 K.

samples can be fitted to the experical power-law equation [17,33,38,39]

$$f_m = A\left(\frac{T - T_g'}{T_g'}\right)^r \quad (3)$$

where T_g' is the zero relaxation frequency temperature, r the exponent and A is a constant. In the above equation it is used as a fitting parameter and has so far been proved to have no physical meaning. However, Eq. (3) is still used here as it is found [38,39] to be a better representative of the data for the supercooled region as compared to William–Landel–Ferry (WLF) or Vogel–Fulchers–Tammanns (VFT) equation. Though the range of f_m values is very limited for CP.OH and NP.OH, the purpose of such a fit is to show that the temperature corresponding to the freezing of the main relaxation process actually corresponds to T_g(pc) measured by the DSC technique. This is shown in Table 4; (although there is some uncertainty in the calculated T_g(pc) as the f_m values are not available over a wider temperature, especially

Table 4
Details of the primary relaxation data in Eq. (3)[a]

Sample	T_g(pc)	T_g'	r	log A (Hz)	T_g(pc) (calc.)[b]
CP.OH	128.5	100	12.97	4.13	128.2
NP.OH	139.3	125	11.31	6.22	144.1
DMCH	107.8	100	10.68	10.81	105.2
CH.OH	150.8	139	8.94	7.35	148.7

[a]All temperatures in degrees Kelvin.
[b]Extrapolated temperature at which $f_m = 10^{-3}$ Hz in Eq. (3).

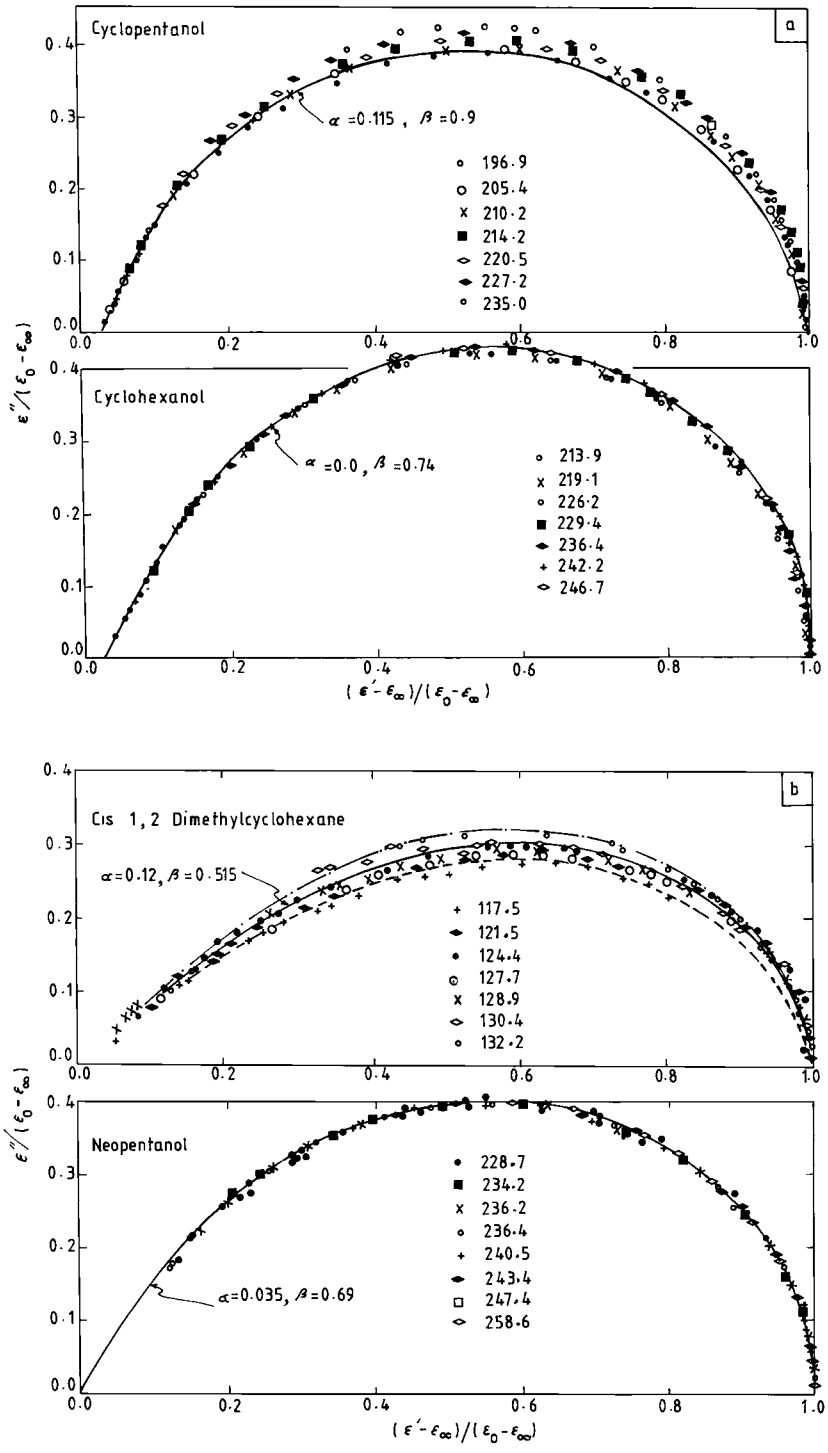

Fig. 3. Normalized C–C plots at different temperatures for: (a) CP.OH and CH.OH; (b) NP.OH and DMCH in the plastic crystalline phase and its supercooled state. The thick lines correspond to Eq. (2) with the corresponding parameters shown along the curves.

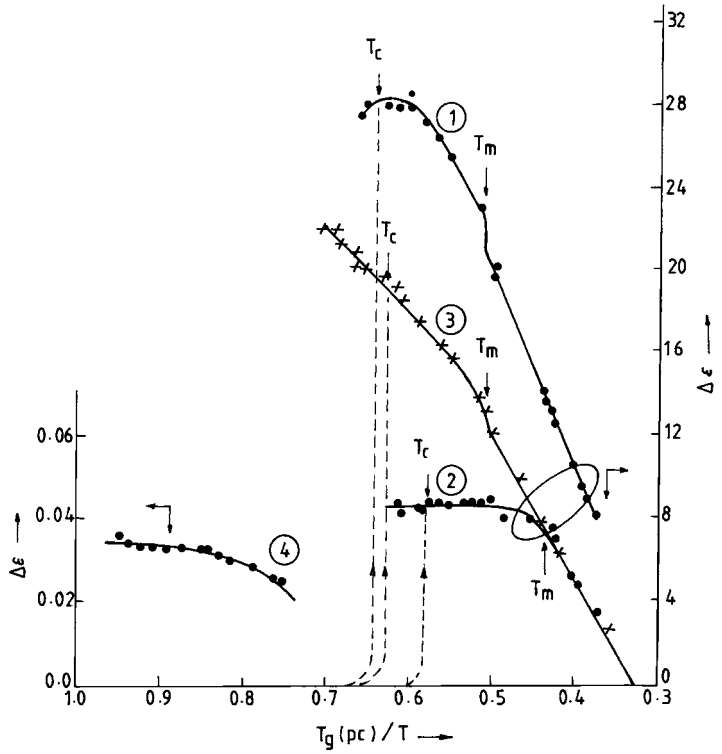

Fig. 4. Variation of dielectric strength $\Delta\epsilon(=\epsilon_0 - 1.05n_D^2)$ against $T_g(\mathrm{pc})/T$. The curves represent: (1) CP.OH; (2) NP.OH; (3) CH.OH; (4) DMCH. Also included is the data from [20,36,37] for the high temperature side.

in the case of NP.OH). Additional sample-wise details are given in the following subsections.

3.4.1. CP.OH

The stable phase transitions in this material were studied earlier using calorimetric method [22,26,27,40] and were confirmed by the dielectric [17,20,41] methods. There are two aspects of its plastic phase which are not yet clear. One is the $T_g(\mathrm{pc})$ value and the other is the shape of the dielectric spectra. According to the paper by Adachi et al. [22] the plastic phase of this material can be supercooled very easily even at a cooling rate of 3 K/min and the $T_g(\mathrm{pc})$ value is given as 138 K (for a heating rate of 1 K/min). (This value has subsequently been quoted by Johari [19] and Angell et al. [42].) But the earlier dielectric work [17,20] casts some doubt on the glass forming ability of the plastic phase as the material quickly crystallizes to a non-rotator phase below 90 K. So a systematic study of this material is undertaken using DSC method. (Although, the DSC curves taken during cooling, especially with the quench cooling accessory, are not very reliable, as the cooling rate cannot be controlled very well; they are taken for different average cooling rates to support the arguments to be made later. It is with this understanding that the cooling curves should be looked-at while analysing the results.) When the sample is cooled at a rate of 2 K/min, it crystallizes in three steps which can be seen as exothermic peaks on curve 1 of Fig. 1. Curve 2 is the subsequent heating curve which is more or less what is expected for an equilibrium sample for temperatures above the crystallization temperature. By looking at curves 1 and 2 one can identify the crystallization peaks in curve 1 with the corresponding endothermic peaks in the heating curve 2; which are listed in Table 1. On increasing the cooling rate to about 10 K/min, the crystallization from plastic crystal II to rigid crystal III at 179.5 K is suppressed; instead the sample crystallizes at 145 K into a different

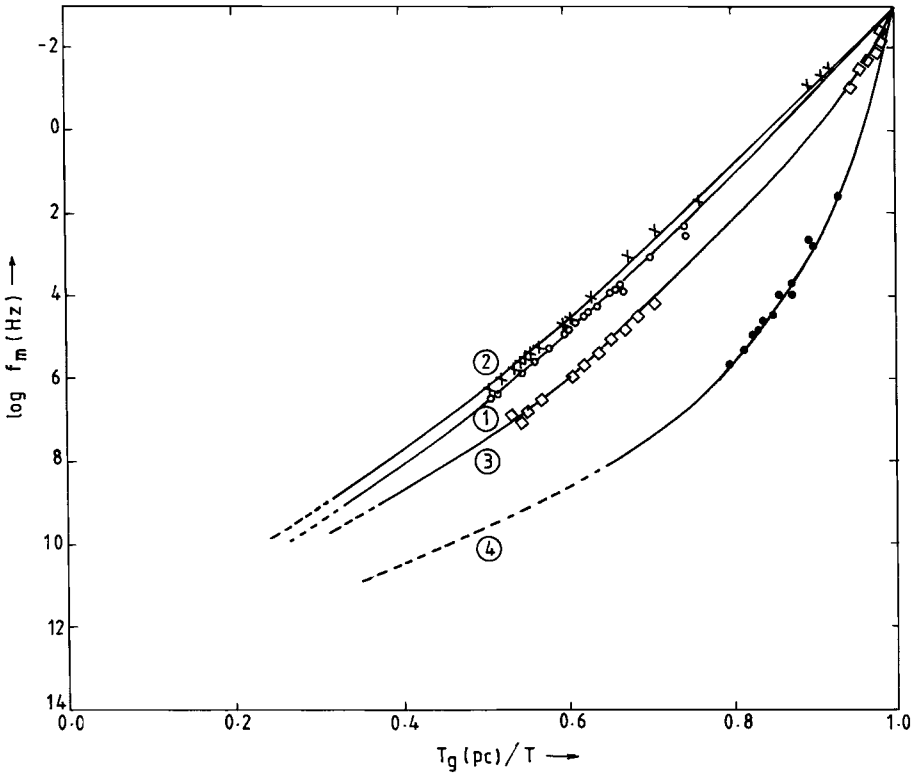

Fig. 5. Variation of $\log f_m$ with $T_g(pc)/T$ for the supercooled plastic phase of: (1) CP.OH; (2) NP.OH; (3) CH.OH; (4) DMCH.

type of rigid crystalline form (crystal IV) (curve 3) which on subsequent heating melts to crystal V at 162 K. This latter crystal immediately gets transformed irreversibly to crystal VI at 168 K (curve 4); which on further heating transforms to stable crystal III at 182 K (curve 5), after which the curve (curve 6) looks more like curve 2. Curve 7 is what one would get if one continues the heating from step 3. No glass transition is observed in these curves, which requires further suppression of crystallization (at 145 K) to a metastable state. This can be achieved by FQC for the plastic phase. This situation is shown in Fig. 2.

The heating curve shown in Fig. 2 is very similar to curve 7 of Fig. 1, except for the crystallization peak starting at 136 K. If the area just below this peak is expanded a small step-like change at 128 K can be clearly seen indicating that the crystallization peak accompanying the glass transition at 128 K is due to the collapse of supercooled crystal II to crystal IV which then undergoes the other (irreversible) transitions as illustrated in Fig. 2. However, the step-like change at T_g in Fig. 2 is very small signifying that a major portion of the sample has already crystallized to crystal IV and crystal III and only a small amount of plastic crystal II is freezing to the glassy state. (An exactly similar DSC curve is obtained for the liquid phase cooled by FQC method indicating that the transformation of liquid to the plastic phase could not be suppressed as required for liquid–glass formation.) This glass transition temperature is confirmed to be due to the freezing of the relaxation process seen in the dielectric method by extrapolating the f_m values to lower temperatures. The value of f_m is found to be of the order of 10^{-3} Hz at 128 K (see Table 4). The DSC curve for CP.OH given by Adachi et al. [22] is similar to the curve 7 of Fig. 1, except for the T_g region. Their curve in this region is suspected because the characteristic crystallization peak following a T_g change (as shown in Fig. 2) is missing in their curve. The dielectric measurements could be followed only upto

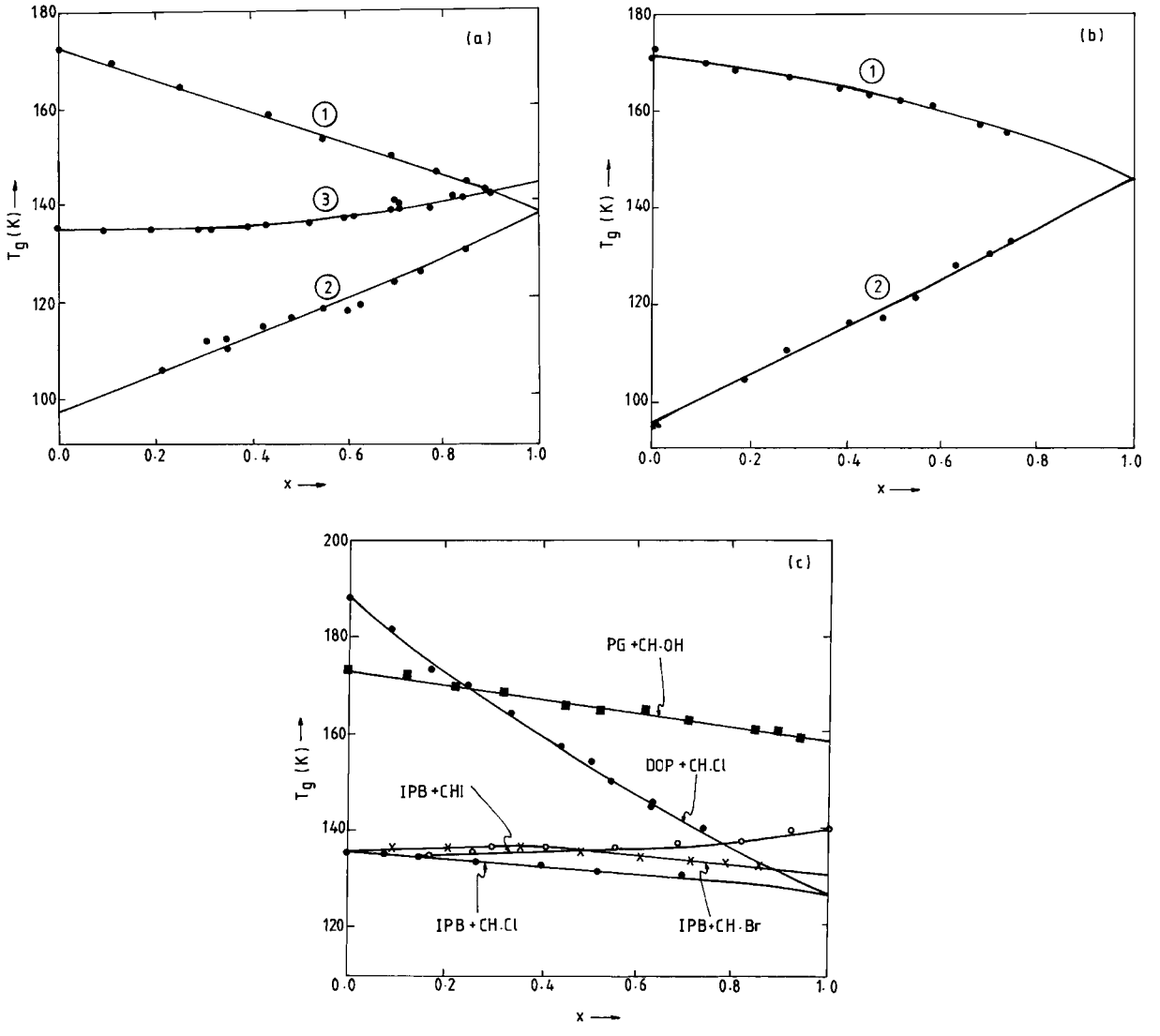

Fig. 6. Variation of the $T_g(l)$ of binary liquids with x. The curves correspond to the binaries of: (a) CP.OH with (1) PG, (2) E.OH and (3) IPB; (b) NP.OH with (1) PG, (2) E.OH; (c) CH.OH, CH.Cl, CH.Br and CH.I. The solid lines are the fits to Eq. (1).

about 10° below the 202 K transition (see Figs. 3 and 4) after which the material collapses to a rigid crystalline state. This situation is shown in Fig. 4. The $T_g(l)$ is obtained by the binary technique and is shown in Fig. 6(a). It is interesting to note that its value is about 9° above $T_g(pc)$. However, the value of $T_g(l)$ obtained with IPB binary is some what higher than that obtained by using PG and EOH. The reason for this is not clear at this moment.

3.4.2. NP.OH

Johari [19] quotes $T_g(pc)$ to be 133 K which is not in agreement with that of Dworkin [21]. The dielectric spectra in the supercooled liquid is quoted [19] to be of Debye type and the temperature dependence of f_m is said to be Arrhenius. This does not appear to be true for the following reasons. When this material from its plastic phase at room temperature is cooled at a rate of about 5 K/min it crystallizes to a non-rotator phase at

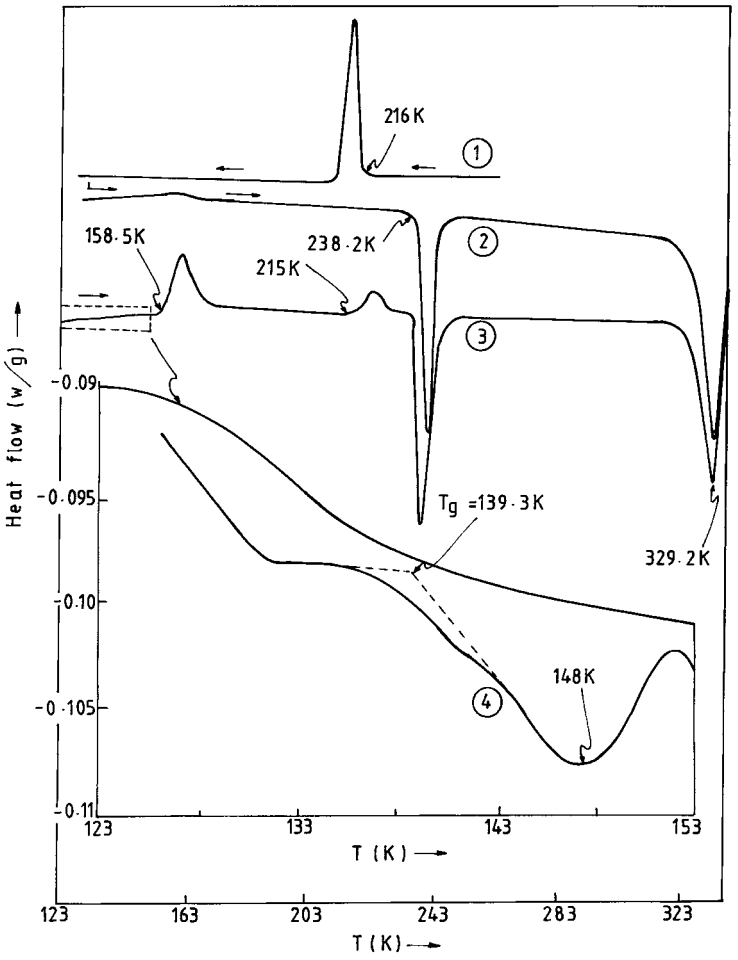

Fig. 7. DSC curves for NP.OH: (1) during cooling at a rate of 5 K of the plastic crystalline phase (from room temperature); (2) corresponding heating curve for a rate of 10 K/min (sample size=15.9 mg); (3) the heating curve at a rate of 10 K/min after the sample is FQC from room temperature (sample size=22.6 mg); (4) (inset) the blown-up portion of curve 3 around the T_g(pc).

216 K; which transforms irreversibly to the plastic phase at 238.2 K on subsequent heating (the curves 1 and 2 of Fig. 7). This is confirmed by the dielectric measurements (Fig. 4) where the dielectric dispersion disappears during supercooling of the plastic phase by about 8°. (The sample melts completely at 329.2 K. The melting curve in the DSC is not sharp and often showed a bifurcation into two melting endotherms, one at 325 K and another ending at 329.2 K, whose magnitudes are found to be sample-history dependent. Probably, the transition at 325 K is a metastable one as it is not found in the samples that are kept at room temperature for several days.) When the plastic phase is cooled using FQC method and then heated, the sample crystallizes into a metastable phase at 158.5 K. This metastable phase later collapses exothermically to a stable phase at 215 K which finally transforms to plastic crystal I at 238.2 K. On closer examination of the DSC curve, as shown in Fig. 7 one can find a small T_g at 139.3 K followed by a small crystallization peak at 148 K. Thus, it appears that a major portion of the material crystallizes during cooling into two different rigid crystalline forms, one of which is metastable with only a small portion of the plastic phase getting transformed into the glassy phase. The extrapolation of the f_m values to lower temperatures yields a T_g(pc)

(calc.) value of 144 K which is closer to that of the DSC finding. The dielectric spectrum is clearly non-Debye for the plastic phase (Fig. 3). The $T_g(l)$ value obtained from the binary solution data shown in Fig. 6(b) is found to be 145.5 K which is about 6–7° above $T_g(pc)$ obtained by the DSC technique.

3.4.3. DMCH

The calorimetric study by Huffman et al. [5] showed that this material exists in plastic crystalline phase I below 223 K and the plastic crystalline phase can be supercooled very easily without any crystallization to a stable rigid crystal II (which occurs [5] at 172.5 K after many days) and shows a glass transition temperature ($T_g(pc)$) at 94 K. The DSC curve taken for this material at a rate of 2 K/min shows (Fig. 8) a $T_g(pc)$ at 105.4 K which is 11° above that of Huffman et al. [5] and melts to a liquid at 224.5 K which agrees with the observations of Huffman et al. [5]. Though, the large difference in the above two $T_g(pc)$ values can partly be accounted for by the prolonged equilibration times used by Huffman et al. [5]; the actual cause is not known. The present dielectric measurements also support the above value of $T_g(pc)$ (see Table 4). The dielectric relaxation in this material was not studied before probably because this material was thought to be nearly non-polar. However, because of the presence of two $-CH_3$ groups in 1,2 positions on the cyclohexane ring, this material acquires a small polarity which amounts to a dielectric strength of about 0.03 (Fig. 4). On using Onsager's formula [18] it gives a dipole moment of approximately 0.08 Debye units. The T-dependence of f_m is strongly non-Arrhenius, and this dielectric process smoothly freezes around 105 K (Table 4). The dielectric relaxation spectrum is very broad and follows Eq. (2) with large value of α (see Fig. 3(b)). The $T_g(l)$ for this liquid is not studied due to constraints on the sample size and its volatility.

3.4.4. CH.OH

This was very well studied using calorimetric [3] and dielectric [6,16,43,44] techniques. However, the shape of the dielectric spectra is not given in the

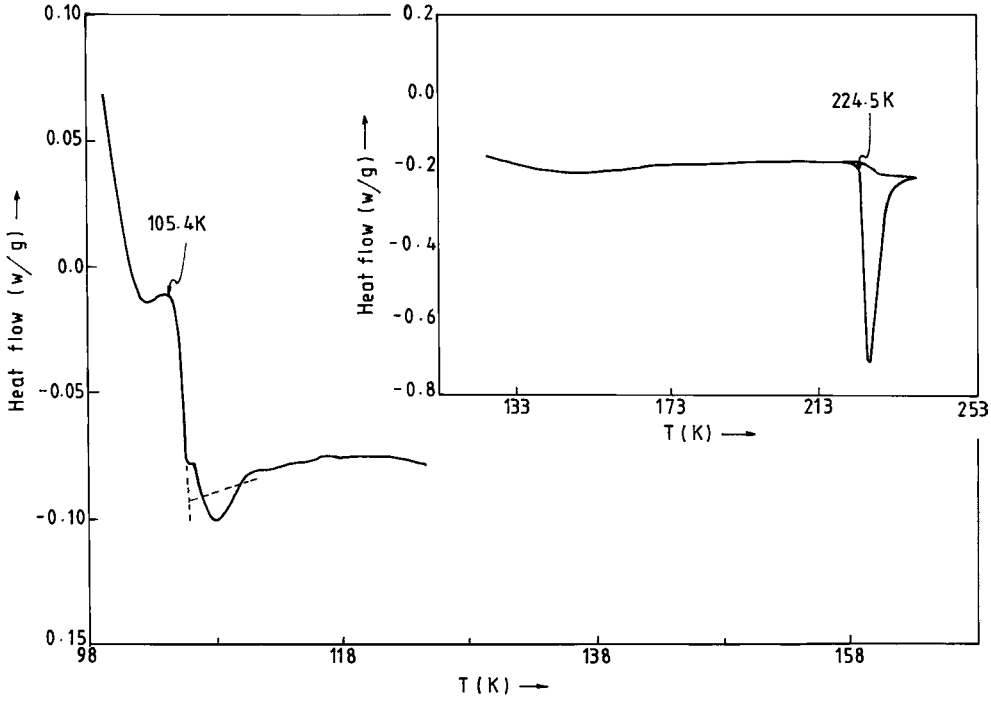

Fig. 8. DSC curve for a heating rate of 2 K/min for the supercooled plastic crystalline phase of DMCH (sample size=20 mg). The inset shows the heating curve for the same sample at temperatures well above $T_g(pc)$ (which shows only the melting transition).

previous publications and hence, is given in Fig. 3(a). The plastic phase could be studied much deeper into the supercooled region (Fig. 4) as compared to CP.OH and NP.OH. The $T_g(l)$ value is measured using PG as the solvent, and is shown in Tables 3 and 4; and is more or less in agreement with the value given by Angell et al. [24].

3.4.5. CH.Cl

This was studied well using both calorimetric [27,28,40] and dielectric [20,41] methods. The reported transition temperatures and the associated enthalpies match with that of the present work (Table 1). This material is not known to supercool very well [40,41]. This situation is shown in Fig. 9. The liquid crystallizes

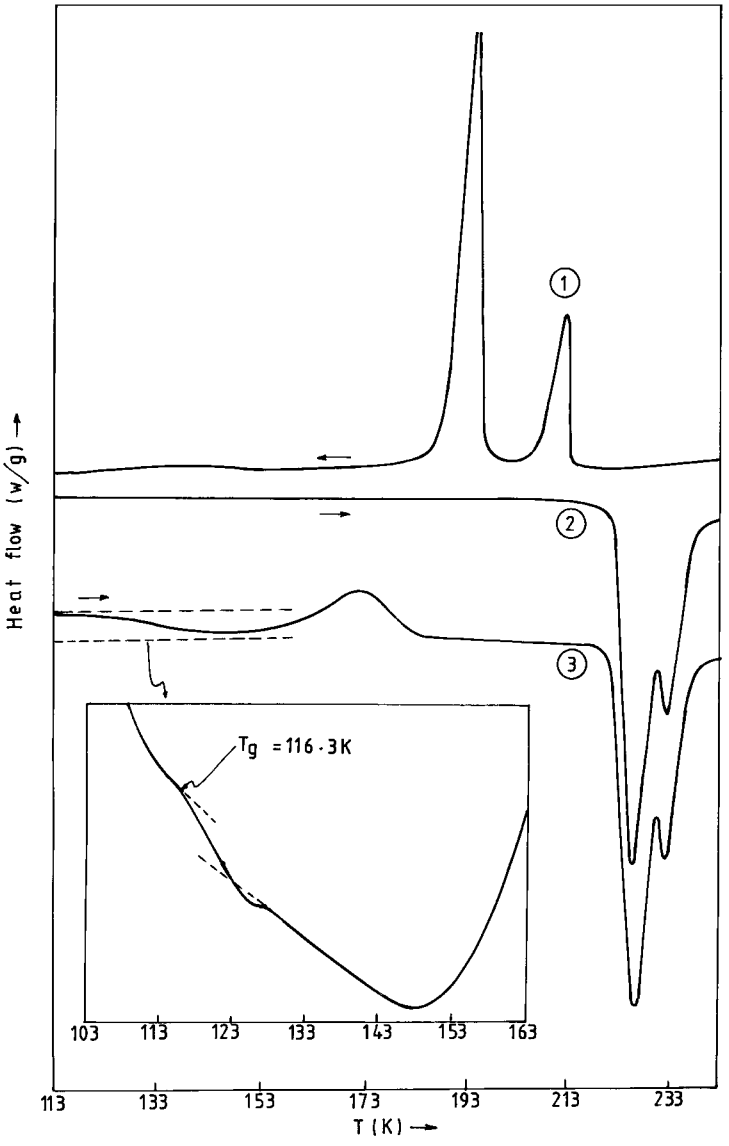

Fig. 9. DSC curves at a rate of 10 K/min in CH.Cl: (1) during cooling; (2) the same sample during heating (sample size=11.2 mg); (3) during heating for a sample which is FQC (sample size=15.2 mg) from its plastic phase. The inset shows the blown-up portion of the T_g(pc) region.

in two steps during slow cooling and which on subsequent heating melts in two steps as expected from the previous studies [40,41]. However, when the sample from the plastic phase is cooled using FQC method, it exhibits (curve 3) a small glass transition event at 116.3 K followed by a two-step crystallization into a metastable form around 165–170 K, which then transforms irreversibly to the stable crystal II phase. The 'glass' formation is only partial in this case. The liquid–glass transition temperature (T_g(l)) is measured using the binary solution method and these results are shown in Fig. 6(c). The dielectric measurements did not yield any new information as the dispersion of the plastic phase is located at much higher frequencies.

3.4.6. CH.Br

This material is not known to crystallize into cubic phase [45] and its crystalline phase is known to be of the non-rotator type [41]. Hence, only one liquid–solid transition is expected which is what is observed in the DSC experiments during slow rate of cooling and heating (Fig. 10). However, when the liquid is cooled

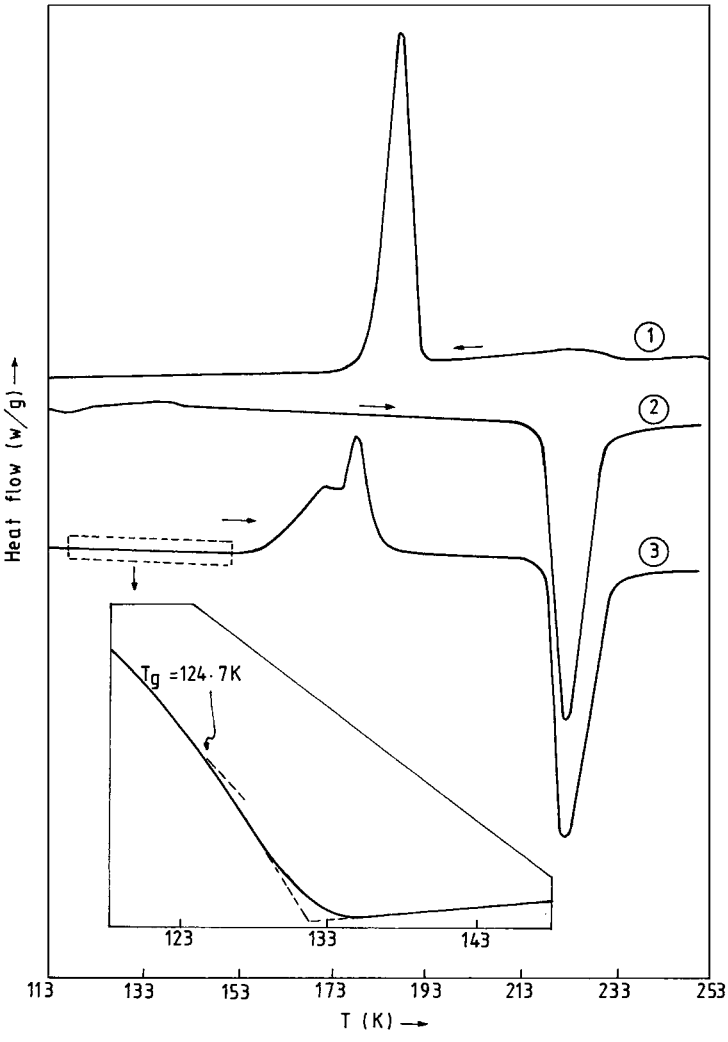

Fig. 10. DSC curves for CH.Br: (1) during cooling at a rate of 10 K/min; (2) same sample during heating at a rate of 10 K/min (sample size=15.9 mg); (3) during heating at a rate of 10 K/min for a sample which is FQC (sample size=18.3 mg). The inset shows the magnified portion of the DSC curve around T_g(pc).

very fast using FQC method, one observes a T_g at 124.7 K followed by two crystallization peaks as shown in curve 3 of Fig. 10. This behaviour is very similar to that of CH.Cl described above. And also the $T_g(l)$ value determined from the binary solution data (Fig. 6(c)) is about 6° above the above T_g of 124.7 K. Therefore it is speculated that CH.Br when cooled very fast, first crystallizes to a metastable crystal II phase which is plastic and which can also be supercooled (to show a $T_g(pc)$ at 124.7 K). On heating it transforms to another metastable crystal phase III which then (irreversibly) transforms to a stable nonrotator phase I and ultimately melts at 217 K. The dielectric method is not found to yield new information as the material quickly crystallizes in the dielectric cell.

3.4.7. CH.I

This liquid crystallizes to a non-rotator phase solid and shows strong (but partial) liquid–glass transition at 139.3 K even for ordinary cooling rates (Fig. 11). On increasing the cooling rate further, no deviations from the above result is observed. The binary solution data clarifies that the above value corresponds to the liquid–glass transition (Fig. 6(c)). The dielectric measurements are not found to yield any extra information as the cooling rate associated with the dielectric cell is not high enough to avoid crystallization.

In addition to the above materials, CH.O is also tested for supercooling of plastic phase. No glass transition is noticed even for very high cooling rates using FQC. The binary solution data gives a $T_g(l)$ of 126 K (Table 2) and all the other parameters measured using DSC technique are entered in Table 1.

4. Discussion and conclusions

For convenience of the discussion the results are presented in the form of a list.

1. *Glassy liquid vs. glassy crystal*: The most interesting result of the present work is that the value of $T_g(l)$ is placed above $T_g(pc)$ by about 6–9°.

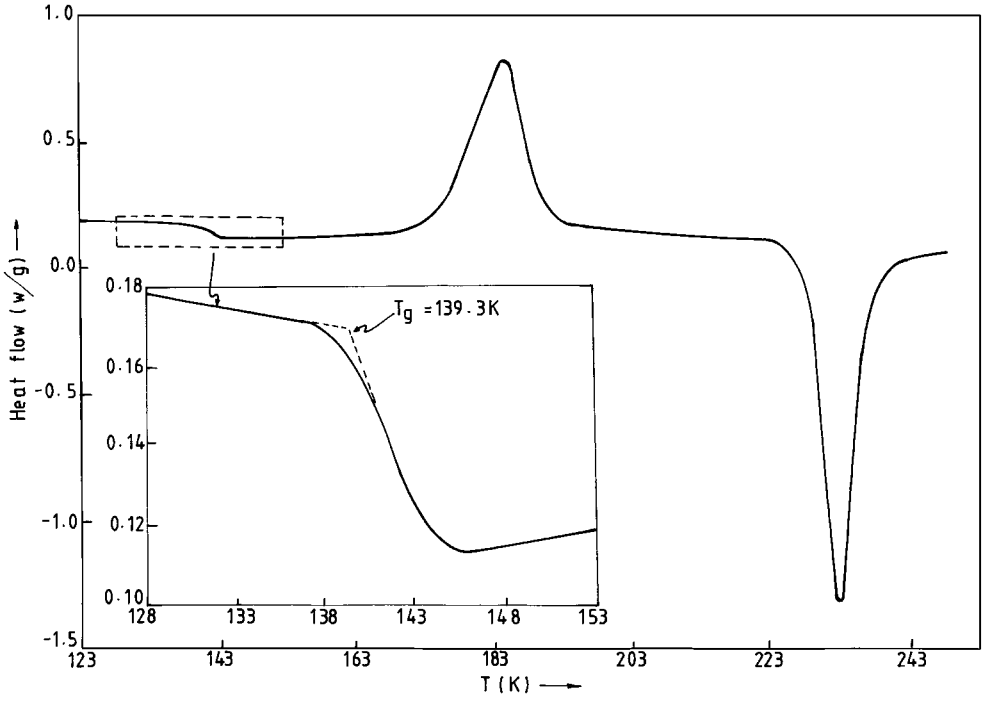

Fig. 11. DSC curve for a sample of CH.I cooled at a rate of 10 K/min (sample size=8.7 mg). The inset shows the magnified portion of the DSC curve in the region of $T_g(l)$.

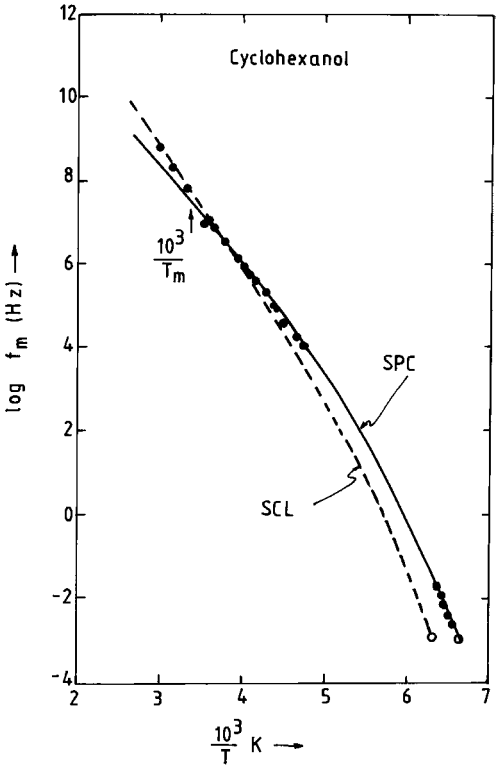

Fig. 12. Variation of the f_m values with temperature for both the liquid [43,44] and plastic crystalline phases. The points shown as ⊙ correspond to the $T_g(l)$ and $T_g(pc)$ values where the corresponding f_m value for the structured relaxation is approximately 10^{-3} Hz.

Interestingly enough in many of the substances [10,46] the $\log f_m$ vs. $1/T$ curves above T_m have a greater slope than that of the corresponding one in the plastic phase just below T_m. Relaxation data are shown in Fig. 12 corresponding to both the liquid and plastic phases for CH.OH. Interestingly, the $\log f_m$ vs. $1/T$ curves appear to take two different routes ending-up at $T_g(l)$ and $T_g(pc)$, respectively, where the corresponding structural relaxation frequencies are of the order of 10^{-3} Hz indicating clearly that the two kinds of aggregation are different. (The situation shown in Fig. 12 is what is expected for the rest of the samples studied here, although the relaxation data corresponding to the liquid phase of these samples is not available.) However, this result is different from the case of ethanol [9,10], where the curve of $\log f_m$ vs. $1/T$ for the supercooled plastic phase lies below that of the liquid phase with both the curves approaching each other in the vicinity of T_g. It may be noted that the difference between $T_g(l)$ and $T_g(pc)$ is not much emphasizing once again the importance of rotational degrees of freedom in these materials as the dominant contributor to the structural relaxation near T_g.

2. It can also seen from Table 2 that the suggested [42] criterion for good glass formation, viz. $T_b/T_m > 2.0$ for liquid–glass and $T_m/T_c > 2.5$ for glassy crystals is in general not violated. The same trend can also be seen in the $T_m/T_g(l)$ or $T_c/T_g(pc)$ values which are mostly above a value of 1.6; whereas, for a good glass former it is typically around 1.35–1.40 in molecular liquids [7]. This behaviour conforms to what is expected from the molecular shape [7] of the substances. For example, replacing one H-atom on the cyclohexane ring by a big atom as iodine I, leads to a good glass former, as the iodine molecule blocks the free rotation of the cyclohaxane ring. On replacing iodine atom with a smaller Cl atom, the resultant increase in molecular symmetry leads to plastic crystal formation on freezing, indicating a decoupling of the positional- and rotational-degrees of freedom. At this point CH.Br appears to be at the threshold of the transition from non-rotator to the rotator phase solids. However, not much could be gathered about the criteria for the glassy crystal formation in the present study. It appears that a glassy crystal formation is much more difficult than a glassy liquid formation, as indicated by the fact that many of the rotator phase solids do not form glassy crystals even for very high cooling rates (e.g. CH.O, etc.).
3. The supercooled plastic phases exhibit strictly non-Arrhenius relaxation as shown in Fig. 5 and follow more or less the general pattern of strong and fragile characteristic stated by Angell [47,48] with increasingly non-Arrhenius materials being increasingly non-Debye too. This can be deduced from the C–C plot given in Fig. 3. The greater fragility character of DMCH can also be seen in its specific heat data [5] which shows a large change at T_g as compared to that of CH.OH [3].
4. From Fig. 4, it may be noted that the $\Delta\epsilon$ values do not vary as $1/T$ in NP.OH and DMCH which is expected for freely rotating dipoles, indicating a

highly restricted rotational freedom in the plastic phase; although one cannot rule out the possibility of increasing tendency for an antiferroelectric arrangement during cooling.

References

[1] J. Wong, C.A. Angell, Glass Structure by Spectroscopy, Marcel Dekker, New York, 1976.
[2] D. Turnbull, Contemp. Phys. 10 (1969) 473.
[3] K. Adachi, H. Suga, S. Seki, Bull. Chem. Soc. Jpn. 41 (1968) 1073.
[4] K. Adachi, H. Suga, S. Seki, S. Kubota, S. Yamaguchi, O. Yano, Y. Wada, Mol. Cryst. Liquid Cryst. 18 (1972) 345.
[5] H.M. Huffman, S.S. Todd, G.D. Oliver, J. Am. Chem. Soc. 71 (1949) 584.
[6] M. Sorai, S. Seki, Mol. Cryst. Liquid Cryst. 23 (1973) 299.
[7] S.S.N. Murthy, Gangasharan, S.K. Nayak, J. Chem. Soc., Faraday Trans. 89 (1993) 509.
[8] H. Suga, S. Seki, J. Non-cryst. Solids 16 (1974) 171.
[9] M.A. Miller, M. Jimenez-Ruiz, F.J. Bermejo, N.O. Birge, Phys. Rev. B 57 (1998) R13977.
[10] S. Benkhof, A. Kudlik, T. Blochowicz, E. Rössler, J. Phys.: Condens. Matter 10 (1998) 8155.
[11] D.L. Leslie-Pelecky, N.O. Birge, Phys. Rev. B 50 (1994) 13250.
[12] R. Brand, P. Lunkenheimer, A. Loidl, Phys. Rev. B 56 (1997) R5713.
[13] J.P. Amoureux, M. Costelain, M.D. Benadda, M. Bee, J.L. Sauvajol, J. Phys. 44 (1983) 513.
[14] J.P. Amoureux, G. Noyel, M. Foulon, M. Bee, L. Jorat, Mol. Phys. 52 (1984) 161.
[15] K. Pathmanathan, G.P. Johari, J. Phys. C 18 (1985) 6535.
[16] Gangasharan, S.S.N. Murthy, J. Chem. Phys. 99 (1993) 9865.
[17] M. Shablakh, L.A. Dissado, R.M. Hill, J. Chem. Soc., Faraday Trans. 79 (1983) 369.
[18] S.S.N. Murthy, J. Phys. Chem. 100 (1996) 8508.
[19] G.P. Johari, Ann. NY Acad. Sci. 276 (1976) 117.
[20] G. Corfield, M. Davies, Trans. Faraday Soc. 60 (1964) 10.
[21] A. Dworkin, Discussions Faraday Soc. 69 (1980) 288.
[22] K. Adachi, H. Suga, S. Seki, Bull. Chem. Soc. Jpn. 43 (1970) 1916.
[23] O. Haida, H. Suga, S. Seki, J. Chem. Thermodyn. 9 (1977) 1133.
[24] C.A. Angell, J.M. Sare, E.J. Sare, J. Phys. Chem. 82 (1978) 2622.
[25] S.S.N. Murthy, A. Paikaray, N. Arya, J. Chem. Phys. 102 (1995) 8213.
[26] A. Wurflinger, J. Kreutzenbeck, J. Phys. Chem. Sol. 39 (1978) 193.
[27] A.R. Ubbelohde, The Molten State of Matter, Wiley, Chichester, UK, 1978.
[28] V.V. Diky, G.J. Kabo, A.A. Kozyro, A.P. Krasulin, V.M. Sevruk, J. Chem. Thermodyn. 26 (1994) 1001.
[29] R.C. Weast, M.J. Astel, Handbook of Physics and Chemistry, CRC Press, 65th Edition, Boca Raton, FL, 1995.
[30] E. Jenckel, R. Heusch, Z. Kolloid 130 (1958) 89.
[31] A.V. Lesikar, Phys. Chem. Glasses 16 (1975) 83.
[32] S.S.N. Murthy, Deepak Kumar, J. Chem. Soc., Faraday Trans. 89 (1993) 2423.
[33] S.S.N. Murthy, J. Phys. Chem. B 101 (1977) 6043.
[34] S.S.N. Murthy, Cryobiology 36 (1998) 84.
[35] S. Havriliak, S. Negami, J. Polym. Sci. C 14 (1966) 99.
[36] F. Buckley, A.A. Maryott, Tables of dielectric dispersion data for pure liquids and dilute solutions, NBS Circular No. 589, 1958.
[37] W. Dannhauser, L.W. Bahe, R.Y. Lin, A.F. Flueckinger, J. Chem. Phys. 43 (1965) 257.
[38] S.S.N. Murthy, J. Chem. Soc., Faraday Trans. II 85 (1989) 581.
[39] S.S.N. Murthy, J. Phys. Chem. 93 (1989) 3347.
[40] G.J. Kabo, V.V. Diky, A.A. Kozyro, A.P. Krasulin, V.M. Sevruk, J. Chem. Thermodyn. 27 (1995) 953.
[41] A.H. White, W.S. Bishop, J. Am. Chem. Soc. 62 (1940) 8.
[42] C.A. Angell, L.E. Busse, E.I. Cooper, R.K. Kadiyala, A. Dworkin, M. Ghelfenstein, H. Szware, A. Vassal, J. Chem. Phys. 82 (1985) 267.
[43] S.K. Garg, C.P. Smyth, J. Chem. Phys. 46 (1967) 373.
[44] N. Pingel, U. Poser, A. Wurflinger, J. Chem. Soc., Faraday Trans. I 80 (1984) 3221.
[45] W.J. Dunning, in: J.N. Sherwood (Ed.), The Plastically Crystalline State, Wiley/Interscience, New York, 1979 (Chapter 1).
[46] N.E. Hill, W.E. Vaughan, A.H. Price, M. Davies, Dielectric Properties and Molecular Behaviour, Van Nostrand Reinhold, London, 1969.
[47] C.A. Angell, W. Sichina, Ann. NY Acad. Sci. 276 (1976) 53.
[48] C.A. Angell, J. Non-cryst. Solids 13 (1991) 131–133.